Resonant photoelectron spectroscopy at the Mo $4p \rightarrow 4d$ absorption edge in MoS_2

Jeffrey R. Lince and Stephen V. Didziulis
Chemistry and Physics Laboratory, The Aerospace Corporation, 2350 E. El Segundo Blvd., El Segundo, California 90245

Jory A. Yarmoff
Department of Physics, University of California at Riverside, Riverside, California 92521
(Received 28 September 1990)

A systematic study has been conducted of the resonant behavior of the valence-band photoelectron spectrum of MoS_2 for $h\nu = 26-70$ eV, spanning the Mo $4p \rightarrow 4d$ transition region. A broad Fano-like resonance appears at ~ 42 eV in the constant-initial-state (CIS) intensity plot of the d_{z^2} peak near the valence-band maximum [~ 2 eV binding energy (BE)], confirming its predominantly Mo $4d$ character. A second shoulder on the higher-$h\nu$ side of the maximum in the d_{z^2} CIS intensity plot is suggested to result from transitions to unoccupied states in the $5sp$ band ~ 10 eV above E_F, by comparison with a partial-yield spectrum and previous inverse-photoemission data. The region of the valence band in the range 3–4.5-eV BE also exhibits resonant behavior, indicating Mo $4d$ character, although somewhat less than for the d_{z^2} peak. The 5–7-eV BE range does not exhibit resonance behavior at the Mo $4p$ edge and, therefore, contains negligible Mo $4d$ character. A feature at ~ 30 eV in the CIS intensity plot for the 5–7-eV BE range could not be definitively assigned in this study, but may be due to a resonance between direct photoemission and a process involving absorption and autoionization of electronic states that contain Mo $5s$ and $5p$ character.

I. INTRODUCTION

The electronic structure of the layered transition-metal dichalcogenide MoS_2 has been examined extensively over the last 20 years. Theoretical studies have used band-structure calculations[1,2] and molecular-orbital (MO) treatments,[3,4] while experimental studies have included angle-resolved ultraviolet photoelectron spectroscopy (ARUPS),[2,5] angle-resolved x-ray photoelectron spectroscopy (ARXPS),[6] angle-integrated ultraviolet photoelectron spectroscopy,[7,8] inverse-photomission spectroscopy (IPES),[9] x-ray-emission spectroscopy (XES),[1,4] and x-ray-absorption spectroscopy (XAS).[10]

Previous experimental studies[2,4,6–8] have indicated that the lowest binding-energy (BE) feature in the valence-band spectrum correlates to the a_1' molecular orbital arising from the Mo $4d_{z^2}$ atomic orbital, which is presumed to be predominantly nonbonding due to limited overlap with S $3p$ orbitals. (The nonbonding nature of this orbital in MoS_2 is caused by its angular nodes, which occur close to the Mo-S internuclear axes.) This assignment is illustrated in Fig. 1, where a valence-band photoelectron spectrum is plotted alongside a generalized MO diagram for MoS_2. (The diagram is determined from a trigonal prism comprised of one Mo atom surrounded by six S atoms, representing one-half of the unit cell of MoS_2 in the hexagonal $2H$ structure.) The remaining levels in the valence-band spectrum have been previously considered to be predominantly S $3p$–based orbitals. The ordering of these S $3p$–based MO's has not been experimentally determined and depends on the bonding interactions of the full S $3p$ orbitals with the empty Mo $4d, 5s, 5p$ orbitals.[3] Only the S $3p$ and $3s$ ligand levels are considered in the bonding schemes because the S $3d$ and higher atomic orbitals are many electron volts above the S $3p$ levels. However, the Mo $5s$ and $5p$ orbitals must be included since they are only 2–6 eV above the Mo $4d$ levels. Symmetry considerations for the D_{3h} point group show that the Mo $4d$ orbitals can mix into MO's having a_1', e', and e'' symmetry, while the Mo $5s$ orbital must mix into a_1' MO's and the Mo $5p$ level will mix with a_2'' and e' MO's (see Fig. 1).[3] This paper explores the

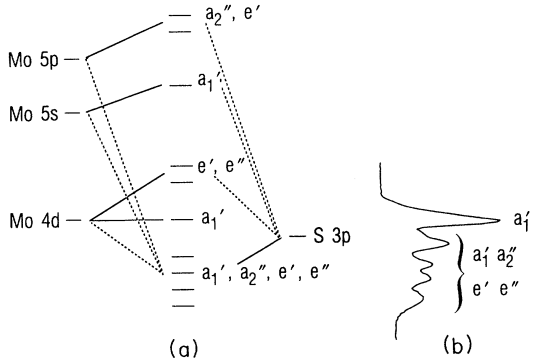

FIG. 1. (a) A generalized molecular-orbital (MO) diagram for MoS_2 (Refs. 3 and 4), plotted on the same (qualitative) energy scale as (b) a valence-band photoelectron spectrum of MoS_2. The spectrum was taken for $h\nu = 60$ eV. The MO diagram is based on an MoS_6 trigonal prism, which represents one-half of the 2H-MoS_2 unit cell. The diagram includes the bonding interactions between the Mo $4d$, $5s$, $5p$, and the S $3p$ orbitals. Symmetry considerations for the D_{3h} point group show that the Mo $4d$ orbitals can mix into MO's having a_1', e', and e'' symmetry, while the Mo $5s$ orbital must mix into a_1' MO's and the Mo $5p$ level will mix with a_1'' and e' MO's.

S $3p$-based levels in more detail by determining the effects of variations of the Mo orbital character on the valence-band photoelectron spectroscopy (PES).

Resonant photoelectron spectroscopy (RPS) has been used increasingly to aid in understanding the photoemission process and to probe the electronic structure of materials.[11] Most of these RPS studies have focused on resonance effects associated with the $3p \rightarrow 3d$ absorption in transition metals and their compounds,[11] especially oxides.[12] However, the utility of RPS in investigating the degree of final-state hybridization, or mixing of atomic levels, in both first-row and higher-row chalcogenides, has recently been demonstrated. For example, RPS was used to reveal considerable metal d and chalcogen p mixing in the valence band of $TaSe_2$ (Ref. 13) and intercalated TiS_2,[14] while the Chevrel-phase Mo_6Se_8 exhibited negligible mixing of these states.[15]

Resonance effects have also been seen for the molybdenum dichalcogenides. In one study, the photon-energy region just below the Mo $4p \rightarrow 4d$ absorption edge of MoS_2 was investigated. The drop in intensity of valence-band peaks at $h\nu = 30-40$ eV was ascribed to an "antiresonance."[7] Resonance effects were also seen in ARUPS of $MoSe_2$,[2] which has an electronic structure very similar to that of MoS_2.

In this paper we present a systematic study of resonance effects in the valence-band spectra of MoS_2 in which we have determined the Mo $4d$ contribution to the various regions of the valence band. The photon energies used (i.e., $h\nu = 26-70$ eV) span the Mo $4p \rightarrow 4d$ absorption edge. The well-defined structure of the MoS_2 valence band allowed for the separation of different resonance behavior occurring in its various BE regions. In general, the results agree with those of the theoretical studies and have clarified the results of the experimental studies.

II. EXPERIMENTAL

Photoelectron spectroscopy was conducted at beam line UV-8b at the National Synchrotron Light Source at Brookhaven National Laboratory. The sample preparation procedures,[16,17] electron spectrometer,[18] and monochromator[19] have been described previously. The design of the angle-integrating electron spectrometer is based on an electrostatic ellipsoidal mirror, which allowed data collection over an area of $\sim \pi/2$ sr, centered approximately about sample normal. Therefore, the valence-band spectra represent an average over the Brillouin zone of MoS_2. The relative intensity of the monochromatized synchrotron radiation was determined by measuring the total current resulting from the electron emission from the (carbon contaminated) Au-coated final focusing mirror with an electrometer. The spectra were normalized by dividing the photoelectron current by the photon intensity determined in this manner in order to cancel the effects of variation in the beam current. The resolution of the system (including contributions from the analyzer and monochromator) was estimated to be 0.3–0.4 eV for the photon-energy range 26–70 eV.

Because of the low-photon energies ($h\nu = 26-70$ eV) and, therefore, low kinetic energies used in the present study, the valence-band spectra represent only the top two molecular layers at the surface (i.e., $\sim 4-6$ deep[20]). However, the $MoS_2(0001)$ surface is virtually bulklike, since it is not reconstructed and exhibits no surface states. The lack of surface states is due to the layered structure of MoS_2: cleavage of the crystal along its van der Waals gap to produce a (0001) surface does not break any covalent bonds.[3]

Clean (0001) surfaces were produced by cleavage of natural molybdenite crystals in air, followed by annealing at ~ 1125 K for 20 min in a sample preparation chamber ($\sim 1 \times 10^{-10}$ Torr base pressure). [The $MoS_2(0001)$ surface does not decompose unless heated to 1300–1400 K.[17]] This annealing procedure is known to remove virtually all contamination from the surface without formation of defects.[21,22] In addition, heating the sample to greater than 923 K removes excess S, if originally present, from the MoS_2 lattice.[23] After annealing, the sample was immediately transferred under vacuum into the spectrometer chamber ($\sim 3 \times 10^{-11}$ Torr base pressure) for analysis. Photoelectron spectra showed sharp Mo $3d$, S $2p$, and valence-band spectra that were indicative of a clean, ordered $MoS_2(0001)$ surface. Under the conditions present in the spectrometer chamber, the highly inert $MoS_2(0001)$ surface could remain clean for a period longer than that required for data collection.

In addition to the valence-band spectra, constant-final-state (CFS) spectra of the $MoS_2(0001)$ surface were taken for detected electron kinetic energies in a window 3 eV wide centered at 10 eV as $h\nu$ was varied from just below the Mo $4p \rightarrow 4d$ absorption edge to 55 eV. An Al foil was used to filter out second- and higher-order light from the monochromator.

III. RESULTS

Valence-band spectra were taken for the following twenty-two photon energies: $h\nu = 26$, 28, 30, 32, 33, 34, 35, 36, 38, 40, 42, 44, 46, 48, 50, 53, 55, 57, 60, 63, 65, and 70 eV. Representative spectra are shown in Fig. 2. As discussed in the Introduction, the lowest binding-energy peak, labeled f, represents an electronic energy level that is primarily Mo $4d_{z^2}$ in character.[3,4,7] Peaks labeled a through e represent regions of the valence band that have varying contributions from Mo and S orbitals. The broad peak at ~ 14 eV represents a predominantly S $3s$ level, but may contain a small amount of Mo character (e.g., Mo $5s$ character[1] and Mo $5p$ character[1,4]). In addition, two broad Auger transitions appear at ~ 15 and ~ 25 eV kinetic energy. Their intensities were negligible, except at higher photon energies for which they appeared at higher BE's than the S $3s$ peak. Therefore, they did not appear to affect our measurement of relative peak areas, as discussed below.

The most conspicuous result shown by Fig. 2 is the large enhancement of peak f in the vicinity of the Mo $4p \rightarrow 4d$ absorption peak, reaching a maximum at ~ 42 eV. There are also discernible changes in the relative intensities of the higher BE peaks (i.e., peaks $a-e$) in the valence band. Peaks c and d also exhibit some enhancement in the same region of $h\nu$ as for peak f. In contrast,

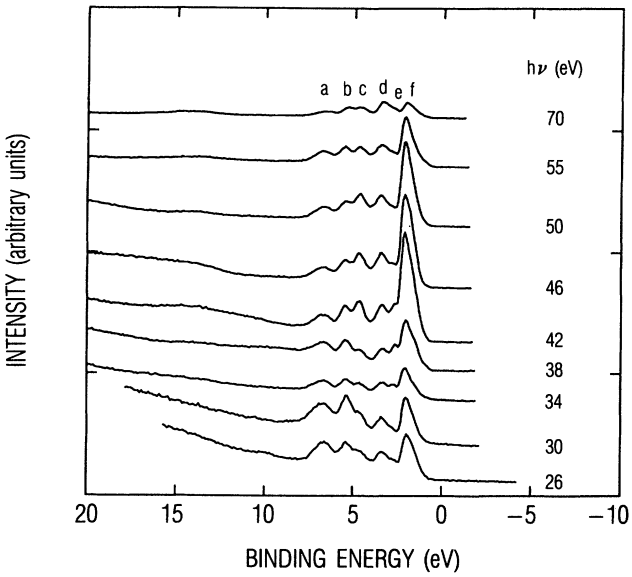

FIG. 2. Valence-band photoelectron spectra of the $MoS_2(0001)$ surface for photon energies that span the Mo $4p \rightarrow 4d$ absorption edge. Only about half of the spectra used in this study are displayed for clarity. The spectra are referenced to the Fermi level (E_F). The S $3s$ peak appears at 14 eV.

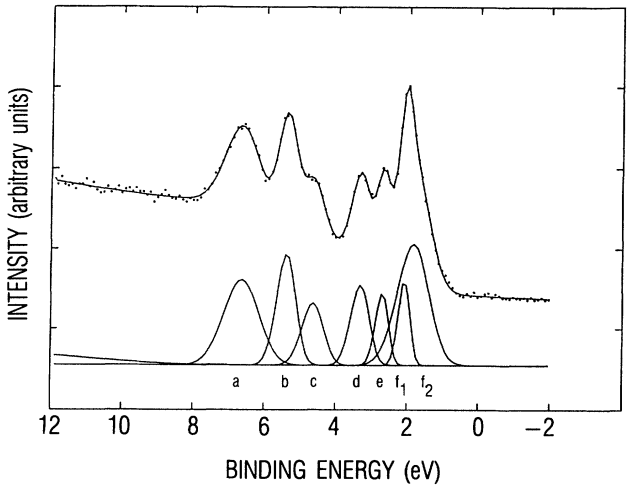

FIG. 3. Peak-fitting results for deconvolution of the $h\nu=36$ eV valence-band spectrum into Gaussians. The raw data are overlaid with the results of the fit in the upper part of the figure. The Gaussian components that make up the fit are shown in the lower part of the figure. The background consists of a Shirley background (Ref. 24) along with a small Gaussian tail. The Gaussian tail can be seen plotted along the left side. The energy positions and widths of the peaks are shown in Table I.

peaks a and b only seem to exhibit enhancement at low values of $h\nu$.

We have investigated these changes in more detail by deconvolution of the valence-band spectra using curve-fitting techniques. We have chosen this method rather than directly measuring constant-initial-state (CIS) spectra because of the partial overlap of neighboring features in the valence-band spectra and the inability of directly measured CIS spectroscopy to remove background effects. The various components of the spectra were determined by fitting with Gaussian peaks (see Fig. 3). The background was approximated by a combination of a Shirley background[24] and a small Gaussian tail.

Initially, the fitting procedure was applied only to the spectra for the following photon energies: $h\nu=26$, 32, 36, 44, 55, 63, and 70 eV. The peak energy positions, widths, and heights were allowed to vary. A mean Gaussian width and a mean energy position were determined for each peak, and these average values were then used for fitting all of the valence-band spectra taken for this study (see Table I). During this second process, only the heights of the peaks were allowed to vary. This procedure minimized effects due to small changes in peak shape, while emphasizing the change in areas of the various peaks. The lack of Gaussian shape of peak f was compensated for by the use of two Gaussian peaks, f_1 and f_2.

Areas of the resultant peaks were determined and are plotted versus photon energy in Fig. 4. These plots essentially represent CIS spectra. The resonance behavior of peak f, the d_{z^2} peak, is seen by the presence of a broad Fano-like resonance[11] in its CIS intensity plot, reaching a maximum at ~42 eV. Additionally, the CIS intensity plot for peak f is enhanced at ~50 eV, and exhibits a small peak at ~31 eV.

These data clarify the results of Ref. 7, in which a dip was seen in the photoelectron intensity of the d_{z^2} peak at ~35 eV for photoelectron spectra taken in the range $h\nu=30$–40 eV. As Fig. 4 shows, this dip is relatively small compared to the subsequently large rise at 38–42 eV. This minimum is due to the Fano line shape, which exhibits a small minimum at photon energies slightly lower than the absorption-edge energy.[11]

Peaks c and d show resonance profiles that are similar to peak f, albeit lower in intensity (see Table II). Peaks a and b do not exhibit the broad resonance beginning at $h\nu=$ ~42 (see Table II), but do exhibit $h\nu=30$ eV peaks of greater intensity than for the other valence-band

TABLE I. Energies and widths of Gaussian peaks used in deconvolution of valence-band spectra.

Peak designation[a]	Binding energy (eV)	Gaussian FWHM[b] (eV)
a	6.63	1.30
b	5.44	0.62
c	4.63	0.89
d	3.36	0.80
e	2.74	0.39
f_1	2.10	0.43
f_2	1.81	0.97

[a]See Fig. 3.
[b]Full width at half maximum.

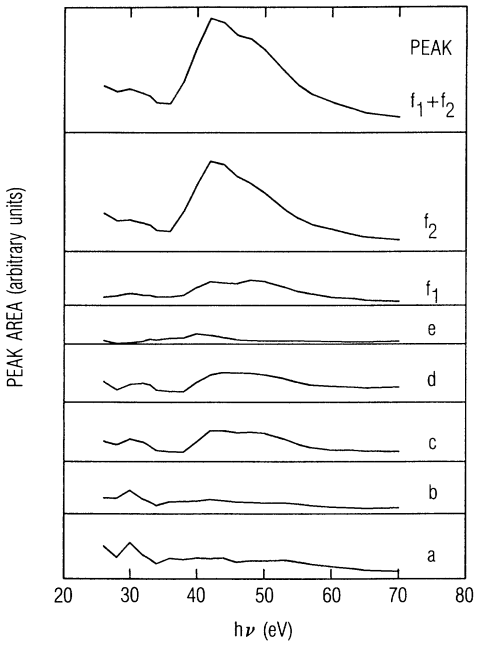

FIG. 4. CIS intensity plots for photon energies spanning the Mo $4p \rightarrow 4d$ absorption edge in MoS_2. The curves were produced by calculating the areas under Gaussian peaks determined from peak-fitting (see Fig. 3). The horizontal line under each curve represents zero intensity for that curve. All curves are on the same scale. The percentage enhancements of each peak measured through the edge are shown in Table II. The peak designations are shown in Figs. 2 and 3.

peaks. The CIS intensity plot for peak *e* has a maximum at 40 eV, but the width is considerably smaller than for peaks *c*, *d*, and *f*.

Note that we found no evidence for either shake-up peaks or satellites in the valence-band PES. (The lack of shake-up processes in the valence band is also supported by the absence of shake-up peaks in the core-level spectra.[17]) The resonant enhancement of peaks *c* and *d* is not consistent with resonant enhancement of a satellite in this energy region for two reasons: (1) A resonantly enhanced satellite peak appearing between peaks *c* and *d* would be expected to fill in the valley between them, but the valley is still well defined at $h\nu=42$ eV, when the resonant enhancement is at its maximum. (2) Resonant enhancement of a satellite peak is accompanied by a *reduction* in intensity in another region of the valence band,[11] but no such reduction is seen in the intensities of any peaks in the present study.

TABLE II. Resonant enhancement of peaks in the valence band measured through the Mo $4p \rightarrow 4d$ edge. Resonant enhancements were measured from percentage increases of CIS intensity plots between the pre-edge value at 34–36 eV and the maximum at 40–45 eV.

Peak designation[a]	Resonant enhancement (% increase)[b]
a	36±20
b	74±40
c	215±20
d	177±20
e	158±60
f_1	181±40
f_2	342±20

[a]See Fig. 3.

[b]Uncertainties were estimated based on uncertainty of determining minima and maxima in CIS intensity plots (Fig. 4) in addition to uncertainty of measuring peak areas in valence-band spectra.

A constant-final-state (CFS) spectrum of the $MoS_2(0001)$ surface was taken for a detected electron kinetic energy of 10 eV, and is shown in Fig. 5. This CFS spectrum can also be denoted a "partial-yield spectrum," since the final state at 10 eV consists mostly of secondary electrons, and gives information similar to x-ray-absorption spectra. The 43-eV feature is due to the transition Mo $4p \rightarrow$ Mo $4d$, while the 51-eV feature is due to a transition from the Mo $4p$ level to higher energy unoccupied Mo $5s$ and $5p$ levels (denoted the "Mo $5sp$ band" for the purposes of the present study). These observations are supported by a recent inverse-photoemission spectroscopy (IPES) study in which the IPES spectrum shows a peak ~ 10 eV above the Fermi energy (E_F), in addition to intensity from $4d$ states that peak ~ 1 eV above E_F.[9] Comparison of the IPES with x-ray-absorption spectra for the S K and Mo L_{III} edges[10] indicated that these higher-energy states are primarily Mo $5s$ and/or Mo $5p$ in character, with a small amount of mixing with Mo states.

IV. DISCUSSION

The enhancement of peak *f* can be described as resulting from a resonance between two photon-induced processes that have the same initial and final states. Since peak *f* represents a state that is primarily Mo $4d$ in character, this resonance results from an interference between the direct photoemission process

$$\text{Mo } 4p^6 4d^2 \rightarrow 4p^6 4d^1 + e^-(\epsilon) \quad (1)$$

and the two-step process involving absorption followed by autoionization

$$\text{Mo } 4p^6 4d^2 \rightarrow 4p^5 4d^3 , \quad (2a)$$

$$\text{Mo } 4p^5 4d^3 \rightarrow 4p^6 4d^1 + e^-(\epsilon) , \quad (2b)$$

where ϵ is the energy of the emitted electron.

The maximum of the d_{z^2} resonance at 42 eV is at a higher BE than that expected from the BE of ~ 37 eV (Ref. 25) for the Mo $4p$ core level in MoS_2. This delayed resonance is commonly seen for other transition metal compounds,[12] and has been explained in terms of exchange interaction in the configuration produced after absorption.[11] The large width of the resonance (as compared to the width expected for a theoretical line shape[11])

depends on the nature of the conduction-band states, but also has been explained as being due to solid-state effects.[11]

The partial-yield spectrum (Fig. 5) exhibits peaks at 43 and 51 eV, which correspond well with the energy positions seen for the curve maximum and shoulder on the CIS intensity plot for peak f. This result, with the IPES (Ref. 9) and x-ray-absorption[10] results previously discussed, indicates that the shoulder at ~ 50 eV in the CIS intensity plot for peak f is due to resonance of the direct photoemission process shown in Eq. (1) with a channel involving absorption to unoccupied Mo s,p levels,

$$\text{Mo } 4p^6 4d^2 \rightarrow \text{Mo } 4p^5 4d^2 5(sp)^1 \quad (3a)$$

followed by autoionization,

$$\text{Mo } 4p^5 4d^2 5(sp)^1 \rightarrow \text{Mo } 4p^6 4d^1 + e^-(\epsilon') , \quad (3b)$$

where ϵ' is the energy of the emitted electron ($\epsilon' - \epsilon \approx 8$ eV). The origin of the small pre-edge peak in the CIS intensity plot for peak f (Fig. 4) will be discussed below.

If a shake-up process had occurred, instead of the autoionization in Eq. (3b), it probably would have resulted in a $4d^0 5(sp)^1$ final state,

$$\text{Mo } 4p^5 4d^2 5(sp)^1 \rightarrow \text{Mo } 4p^5 4d^0 5(sp)^1 + e^-(\epsilon'') , \quad (3c)$$

where $\epsilon'' \approx \epsilon$, which would appear 8–10 eV below the corresponding initial state in the valence-band spectrum. The presence of shake-up peaks is common for first-row transition metals as a result of d-d electron repulsion, which favors decay mechanisms involving d electrons, but does not generally occur in second- and third-row transition metals.[26] Therefore, it is not surprising that shake-up does not occur in MoS_2, which, in addition to being in the second transition series, has only two d electrons (Mo is in the 4+ state), so that d-d repulsion is relatively small.

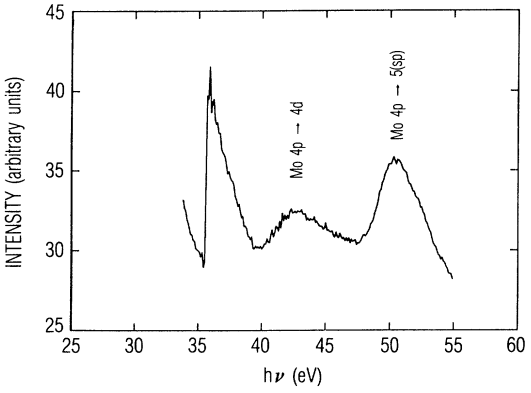

FIG. 5. Partial-yield spectrum (or CFS) of MoS_2 for photon energies spanning the Mo $4p \rightarrow 4d$ absorption edge. This spectrum was produced by measuring the intensity of electrons with 10 eV kinetic energy as the photon energy was ramped. The sharp edge seen at 36 eV is due to cutoff of second-order light from the monochromator by an Al filter.

The conclusion that peak f is predominantly of Mo $4d$ character based on resonant enhancement at the Mo $4p$ edge is in agreement with most studies on the electronic structure of MoS_2 (see Sec. I). However, in an ARUPS study of $MoSe_2$, whose electronic and crystal structure is similar to MoS_2, the existence of a nondispersing excitation involving a "polaronic" state was seen ~ 1 eV below the valence-band maximum (VBM).[2] Existence of this dispersionless transition was not apparent in an ARUPS study of MoS_2,[5] however, the energy resolution may have been poorer than that in Ref. 2. If a transition involving a polaronic state exists for MoS_2, then it would be expected to appear at a BE of ~ 2 eV (i.e., referenced to E_F) in the present study. In addition, the study of Ref. 2 found another dispersionless state in $MoSe_2$ that was predicted to have considerable Mo d character at ~ 1.5 eV below the VBM (i.e., at ~ 2.5 eV referenced to E_F). The need to use two Gaussians (f_1 and f_2) to describe the variation in the peak shape of peak f, and the small widths of peaks e and f_1 (compared to those for peaks a, b, c, d, and f_2), indicates that peaks e and f_1 (at 2.7 and 2.1 eV, respectively) are the dispersionless peaks found in Ref. 2 for $MoSe_2$. The larger width of peak f_2 is consistent with its interpretation as the predominantly d_{z^2} peak at the top of the valence band discussed in the Introduction. The interpretation of peaks e and f_1 as representing transitions involving levels of predominantly Mo $4d$ character is consistent with the observation of their resonant behavior near the Mo $4p \rightarrow 4d$ absorption edge (see Fig. 4). The small width of the CIS intensity plot for peak e may be due to the inability to accurately deconvolute a peak with such a small intensity, or it may be due to the lack of strong coupling to the $5sp$ band due to the localized nature of the electronic level represented by peak e.

The resonance behavior of peaks c and d is consistent with the presence of considerable Mo $4d$ character in these regions of the valence band. In contrast, the lack of the broad resonance between 40 and 60 eV for peaks a and b indicates only a small contribution from Mo $4d$ states. These results allow partial assignment of the valence-band peaks to MO levels (i.e., as the initial states). The Mo $4d$ behavior of peaks c and d indicates that they represent the e' and e'' MO levels, since these levels are expected to contain Mo $4d$ character along with S $3p$ character.[3,4] The lack of $4d$ resonance behavior for peaks a and b is consistent with their representing the a_2'' level and the bonding a_1' level [as opposed to peak f_2, which represents the "nonbonding" $a_1'(d_{z^2})$ level].[3,4] The a_2'' level should contain predominantly S $3p$ and Mo $5p$ character, with negligible Mo $4d$ character, while the bonding a_1' level is expected to contain mostly S $3p$ and Mo $5s$ character, with a small Mo $4d_{z^2}$ contribution.[3,4] The virtual lack of Mo $4d$ resonance behavior in peaks a and b indicates that this $4d_{z^2}$ contribution is small indeed in whichever of these two peaks represents the bonding a_1' level.

These conclusions are in good agreement with the results of Haycock, Urch, and Wiech.[4] They proposed an ordering for the MO levels based on their XES data, which essentially indicated Mo $4d$ character in the low

BE region, S 3p character in the middle and high BE regions, and Mo 4p in the high BE region of the valence band. As a result, they proposed the following ordering (with increasing BE): nonbonding a_1', e'', e', bonding a_1', and a_2''. Their proposal that e' is at higher BE than e'', and that the a_2'' level is at higher BE than the bonding a_1' level, appeared to be motivated by the presence of Mo 5p character in the higher BE region of the valence band. However, XES was not conducted for transitions that might probe other orbitals; for example, Mo 5s, which would certainly affect the ordering of the bonding a_1' and a_2'' levels.

Our results are also qualitatively supported by band-structure calculations. For $MoSe_2$, which is very similar to MoS_2, partial density of states for Mo and Se were determined from augmented-spherical-wave band-structure calculations in Ref. 2, and indicated that Mo 4d character was present in the middle of the valence band, but in decreasing amounts for increasing BE. Results from a self-consistent pseudopotential calculation[1] also indicated Mo 4d character in the middle of the valence band.

Experimental studies, however, have provided differing views on the role of the various atomic contributions to different areas of the valence band. McGovern *et al.*[8] have conducted variable photon-energy studies of the valence band of MoS_2 in the range 60–150 eV, while Abbati *et al.*[7] have conducted a higher resolution study in the range 65–170 eV (in addition to the 30–40-eV range discussed in Sec. I). In both cases, a large drop in intensity of the d_{z^2} peak (peak f in the present study) relative to the other peaks was seen for photon energies of ~70–120 eV due to a broad Mo 4d Cooper minimum (CM) that is centered at ~90 eV.[27] In addition, some evidence is seen for a CM in the rest of the valence band,[7] although the effect is somewhat smaller. In Ref. 7 it was proposed that the highest BE valence-band peak (peak a in the present study) had more Mo 4d character than the middle of the valence band (peaks b, c, and d in the present study), which is in disagreement with our results. However, some of the relative changes in peak intensities may be explained by the presence of atomic orbitals other than Mo 4d and S 3p that also have contributions in the valence band. As discussed above, the XES study of MoS_2, by Haycock, Urch, and Wiech, showed that a significant amount of Mo 5p character was present in the higher BE regions of the valence band.[4] The photoemission cross section for 5p states drops faster than either the Mo 4d or S 3p states as the photon energy is increased at energies just below the CM.[27] After the CM (i.e., for $h\nu > 120$ eV), the PES spectra in Ref. 7 show that the relative intensity of the d_{z^2} peak (peak f) increases somewhat, while the relative intensity of the higher BE peak (peak a) does not appear to recover.[7] Therefore, the relative drop in the intensity of peak a near $h\nu = 90$ eV may be due to its partially Mo 5p character. It should be noted that, as discussed above, some Mo 5s character may also be present in the higher BE valence levels. However, the photoemission cross section for Mo 5s states varies similarly to the S 3p cross section in the range $h\nu = 50$–150 eV,[27] so that they would not cause the difference in behavior between peak a and peaks b, c, and d.

The peak at ~30 eV in the CIS intensity plot (Fig. 4) is more intense for the higher BE regions in the valence band and is especially intense for peak a. The enhancement in peaks a and b is clearly seen in the valence-band spectra in Fig. 2. Some of the changes near $h\nu = 30$ eV may be due to the presence of the S 3p CM, which occurs in the range $h\nu = 27$–40 eV. However, the small width of the CIS feature at 30 eV would tend to favor a resonance-related effect rather than a simple variation in cross section. One possible explanation involves a S $3s \rightarrow$ Mo 5(sp) absorption, which could then proceed to an S-based autoionization involving the levels represented by peaks a and b. This is not as farfetched as it might seem, since there is evidence that there is significant Mo 5s character[1] and Mo 5p character[1,4] in the S 3s level, and in the levels represented by peak a and peak b. However, a definitive assignment of this CIS feature is beyond the scope of the present study. Similar studies of other compounds with well-characterized orbital contributions to the various areas of their valence bands might provide answers to the question of resonances involving ligand levels.

V. CONCLUSIONS

We have conducted a detailed study of the resonance behavior of the valence band of MoS_2 near the Mo $4p \rightarrow 4d$ absorption edge using variable photon-energy photoelectron spectroscopy. Resonance effects in the different regions of the valence band were examined by deconvolution using peak-fitting techniques. The areas under the resultant peaks were displayed as a function of the photon energy to give CIS intensity plots that allowed the determination of the various atomic orbital contributions to molecular orbitals in these regions. The results agree well with theoretical studies involving band-structure calculations and molecular-orbital treatments performed by other groups and helped to clarify results from other experimental studies.

Specifically, we found a broad Mo $4p \rightarrow 4d$ resonance peaking at 42 eV for the CIS intensity plot representing the "Mo d_{z^2}" level near the VBM, confirming that it is predominantly Mo 4d in character. The CIS intensity plots representing the middle of the valence band also exhibited resonant enhancement, although with somewhat less intensity than for the d_{z^2} level, indicating considerable mixing of Mo 4d states with S 3p states. The higher binding-energy region of the valence band did not exhibit the Mo $4p \rightarrow 4d$ resonance, indicating negligible Mo 4d character. However, CIS intensity plots from peaks in this region showed a peak at ~30 eV that may be due to a resonance with an absorption and autoionization involving electronic states with Mo 5s and 5p character.

In addition, we examined resonant effects of two weak features in the valence-band PES spectra, at 2.7 and 2.1 eV binding energies (i.e., at ~1.8 and ~1.2 eV below the VBM, respectively). The large proportion of Mo 4d character, small widths, and energy positions of these peaks

indicate that they are related to a weakly dispersing peak predicted in the band structure of $MoSe_2$, and a nondispersing peak that has been proposed to represent a polaron that exhibits mostly Mo 4*d* character.[2]

ACKNOWLEDGMENTS

This work was supported predominantly by Air Force Systems Command, Space Systems Division Contract No. F04701-88-C-0089. Research was carried out at the National Synchrotron Light Source (NSLS), Brookhaven National Laboratory, which is supported by the U.S. Department of Energy, Division of Materials Sciences and Division of Chemical Sciences (DOE Contract No. DE-AC02-76CH00016). The authors would like to thank R. Kurtz and K. Smith for helpful comments, and F. R. McFeely of IBM Yorktown Research Center and the staff at NSLS for their assistance.

[1]A. Simunek and G. Wiech, Phys. Rev. D **30**, 923 (1984).
[2]R. Coehoorn, C. Haas, J. Dijkstra, C. J. F. Flipse, R. A. De Groot, and A. Wold, Phys. Rev. B **35**, 6195 (1987).
[3]P. D. Fleischauer, J. R. Lince, P. A. Bertrand, and R. Bauer, Langmuir **5**, 1009 (1989).
[4]D. E. Haycock, D. S. Urch, and G. Wiech, Faraday Trans. II **75**, 1692 (1979).
[5]R. Mamy, A. Boufelja, and B. Carricaburu, Phys. Status Solidi B **141**, 467 (1987).
[6]L. Ley, R. H. Williams, and P. C. Kemeny, Nuovo Cimento **39**, 715 (1977).
[7]I. Abbati, L. Braicovich, C. Carbone, J. Nogami, I. Lindau, and U. del Pennino, J. Electron. Spectrosc. Relat. Phenom. **40**, 353 (1986).
[8]I. T. McGovern, K. D. Childs, H. M. Clearfield, and R. H. Williams, J. Phys. C **14**, L243 (1981).
[9]M. Sancrotti, L. Braicovich, C. Chemelli, and G. Trezzi, Solid State Commun. **66**, 593 (1988).
[10]Y. Ohno, K. Hirama, S. Nakai, C. Sugiura, and S. Okada, Phys. Rev. B **27**, 3881 (1983); Y. Ohno, K. Hirama, S. Nakai, C. Sugiura, and S. Okada, J. Phys. C **16**, 6695 (1983).
[11]L. C. Davis, J. Appl. Phys. **59**, R25 (1986).
[12]K. E. Smith and V. E. Henrich, Phys. Rev. B **38**, 9571 (1988).
[13]H. Sakamoto, S. Suga, M. Taniguchi, H. Kanzaki, M. Yamamoto, M. Seki, M. Naito, and S. Tanaka, Solid State Commun. **52**, 721 (1984).
[14]Y. Ueda, H. Negishi, M. Koyano, M. Inoue, K. Soda, H. Sakamoto, and S. Suga, Solid State Commun. **57**, 839 (1986).
[15]H. Namatame, K. Soda, T. Mori, M. Fujisawa, M. Taniguchi, S. Suga, K. Kitazawa, and S. Tanaka, Jpn. J. Appl. Phys. **28**, L266 (1989).
[16]J. R. Lince, T. B. Stewart, M. M. Hills, P. D. Fleischauer, J. A. Yarmoff, and A. Taleb-Ibrahimi, Surf. Sci. **210**, 387 (1989).
[17]J. R. Lince, T. B. Stewart, M. M. Hills, P. D. Fleischauer, J. A. Yarmoff, and A. Taleb-Ibrahimi, Surf. Sci. **223**, 65 (1989).
[18]D. E. Eastman, J. J. Donelon, N. C. Hien, and F. J. Himpsel, Nucl. Instrum. Methods **172**, 327 (1980).
[19]F. J. Himpsel, Y. Jugnet, D. E. Eastman, J. J. Donelon, D. Grimm, G. Landgren, A. Marx, J. F. Morar, C. Oden, and R. A. Pollak, Nucl. Instrum. Methods **222**, 107 (1984).
[20]M. P. Seah and W. A. Dench, Surf. Interf. Anal. **1**, 2 (1979); S. Tanuma, C. J. Powell, and D. R. Penn, Surf. Sci. **192**, L849 (1987).
[21]J. C. McMenamin and W. E. Spicer, Phys. Rev. B **16**, 5474 (1977).
[22]M. Kamaratos and C. A. Papageorgopoulos, Surf. Sci. **160**, 451 (1985).
[23]J. S. Zabinski and B. J. Tatarchuk, in *New Materials Approaches to Tribology: Theory and Applications,* Materials Research Society Symposium Proceedings, edited by L. E. Pope, L. L. Fehrenbacher, and W. O. Winer (Materials Research Society, Pittsburgh, 1989), Vol. 140, pp. 239ff.
[24]D. A. Shirley, Phys. Rev. B **5**, 4709 (1972).
[25]J. R. Lince, T. B. Stewart, P. D. Fleischauer, J. A. Yarmoff, and A. Taleb-Ibrahimi, J. Vac. Sci. Technol. A **7**, 2469 (1989).
[26]G. A. Vernon, G. Stucky, and T. A. Carlson, Inorg. Chem. **15**, 278 (1976).
[27]J. J. Yeh and I. Lindau, At. Data Nucl. Data Tables **32**, 1 (1985).